Leaf Senescence and Starvation-Induced Chlorosis Are Accelerated by the Disruption of an Arabidopsis Autophagy Gene[1]

Hideki Hanaoka, Takeshi Noda, Yumiko Shirano[2], Tomohiko Kato, Hiroaki Hayashi, Daisuke Shibata[3], Satoshi Tabata, and Yoshinori Ohsumi*

Department of Cell Biology, National Institute for Basic Biology, Nishigonaka 38, Myodaiji-cho, Okazaki 444–8585 Japan (H. Hanaoka, T.N., Y.O.); Department of Molecular Biomechanics, School of Life Science, The Graduate University for Advanced Studies, Okazaki 444–8585, Japan (H. Hanaoka, T.N., Y.O.); Mitsui Plant Biotechnology Research Institute (disbanded in March 1999), Tsukuba, Ibaraki 305–0047, Japan (Y.S., D.S.); Kazusa DNA Research Institute, Yana 1532–3, Kisarazu, Chiba 292–0812, Japan (T.K., S.T.); and Department of Applied Biological Chemistry, Graduate School of Agricultural and Life Sciences, The University of Tokyo, 1–1–1 Yayoi, Bunkyo-ku, Tokyo 113–8657, Japan (H. Hayashi)

Autophagy is an intracellular process for vacuolar bulk degradation of cytoplasmic components. The molecular machinery responsible for yeast and mammalian autophagy has recently begun to be elucidated at the cellular level, but the role that autophagy plays at the organismal level has yet to be determined. In this study, a genome-wide search revealed significant conservation between yeast and plant autophagy genes. Twenty-five plant genes that are homologous to 12 yeast genes essential for autophagy were discovered. We identified an Arabidopsis mutant carrying a T-DNA insertion within *AtAPG9*, which is the only ortholog of yeast Apg9 in Arabidopsis (*atapg9-1*). *AtAPG9* is transcribed in every wild-type organ tested but not in the *atapg9-1* mutant. Under nitrogen or carbon-starvation conditions, chlorosis was observed earlier in *atapg9-1* cotyledons and rosette leaves compared with wild-type plants. Furthermore, *atapg9-1* exhibited a reduction in seed set when nitrogen starved. Even under nutrient growth conditions, bolting and natural leaf senescence were accelerated in *atapg9-1* plants. Senescence-associated genes *SEN1* and *YSL4* were up-regulated in *atapg9-1* before induction of senescence, unlike in wild type. All of these phenotypes were complemented by the expression of wild-type *AtAPG9* in *atapg9-1* plants. These results imply that autophagy is required for maintenance of the cellular viability under nutrient-limited conditions and for efficient nutrient use as a whole plant.

Protein degradation is an important process in almost every facet of plant physiology and development. In plants, three major degradation pathways have been described: the ubiquitin-dependent pathway and the chloroplast and the vacuolar degradation pathways (for review, see Vierstra, 1996). Among these pathways, vacuolar degradation is assumed to be involved in bulk protein degradation by virtue of the resident proteases in the vacuole. Two types of vacuoles have been described in plants: the storage vacuole and the lytic central vacuole (for review, see Marty, 1999). However, there may be additional vacuole types that await discovery. Protein storage vacuoles are often found in seed tissues and accumulate proteins that are mobilized and used as the main nutrient resource for germination. Most cells in vegetative tissues have a large central vacuole, containing a wide range of proteases in an acidic environment. Substrate proteins must be transported and sequestered into this vacuole for degradation.

Autophagy, a ubiquitous eukaryotic process, is responsible for this sequestration. Two types of autophagy have been described, namely macroautophagy and microautophagy (for review, see Klionsky and Ohsumi, 1999). In yeast macroautophagy, a portion of the cytoplasm is first enclosed by a double-membrane structure, the autophagosome. The outer membrane of the autophagosome then fuses to the vacuolar membrane, so that its inner membrane structure, the autophagic body, is delivered into the vacuolar lumen. The contents of the autophagic body are then digested by vacuolar proteinases. In animal cells, the lysosome functions as the degradation compartment, and the autophagosome fuses with a lysosome to become an autolysosome. In microautophagy, the vacuolar membrane invaginates to engulf the substrates and is then pinched off. The enclosed cytoplasm is then degraded inside the vacuole.

[1] This work was supported in part by the Grants-in-Aid for Scientific Research from the Ministry of Education, Science, Sports and Culture of Japan.

[2] Present address: Boyce Thompson Institute for Plant Research, Tower Road, Ithaca, NY 14853.

[3] Present address: Kazusa DNA Research Institute, Yana 1532–3, Kisarazu, Chiba 292–0812, Japan.

* Corresponding author; e-mail yohsumi@nibb.ac.jp; fax 81–564–55–7516.

Article, publication date, and citation information can be found at www.plantphysiol.org/cgi/doi/10.1104/pp.011024.

Plant processes analogous to macroautophagy and microautophagy have been described in a number of morphological and biochemical studies (for reviews, see Matile, 1975; Moriyasu and Hillmer, 2000). In rice (*Oryza sativa*)-, sycamore (*Acer pseudoplatanus*)-, and tobacco (*Nicotiana tabacum*)-cultured cells, autophagy is induced by Suc starvation (Chen et al., 1994; Aubert et al., 1996; Moriyasu and Ohsumi, 1996). Net protein degradation is induced by carbon starvation in whole maize (*Zea mays*) plants, most likely by an autophagic process (Brouquisse et al., 1998). In cultured sycamore cells, double-membrane-bound autophagosomes are formed in the cytoplasm and are eventually expelled into the central vacuole (Aubert et al., 1996). In tobacco-cultured cells, the autophagic component is conversely thought to be the autolysosome-like small lytic compartment, rather than the central vacuole (Moriyasu and Ohsumi, 1996).

Autophagy was proposed to be involved in various plant developmental processes such as vacuole formation in root meristematic cells (Marty, 1978), development of cotyledon leaves (Toyooka et al., 2001), and senescence (Matile and Winkenbach, 1971; Inada et al., 1998). Chloroplasts are equipped with a variety of intrinsic proteases that are thought to be responsible for protein degradation during leaf senescence (Musgrove et al., 1989; Bushnell et al., 1993). At the same time, it has been suggested that vacuolar degradation of chloroplasts in senescent leaves also occurs (Wittenbach et al., 1982; Ono et al., 1995; Minamikawa et al., 2001). Thus, although many reports have been published on plant autophagy, how autophagy contributes to plant life is still to be determined. This must be because of a current lack of knowledge regarding genes involved in autophagy and autophagy-related mutant plants.

In the yeast *Saccharomyces cerevisiae*, a group of autophagy-defective mutants (*apg* and *aut*) were isolated (Tsukada and Ohsumi, 1993; Thumm et al., 1994). Most Apg/Aut proteins are directly involved in autophagosome formation, but these mutants possess functionally normal vacuoles. As a consequence of a specific defect in autophagy, all of these mutants display the following phenotypes: a defect in (a) bulk protein degradation induced by starvation, (b) survival during starvation, and (c) diploid cell sporulation. Through characterization of the Apg gene products, several molecular mechanisms essential for yeast autophagosome formation were discovered such as the Tor-Apg1 phosphorylation system, the Apg12 conjugation system, and the Apg8 lipidation system (for reviews, see Klionsky and Ohsumi, 1999; Ohsumi, 2001). Orthologs of most Apg proteins were found in mammalian cells. Several sets of results indicate that the Apg proteins are essential for autophagy in mammals and that the molecular mechanism of autophagy is conserved among the different systems (Mizushima et al., 1998b, 2001; Liang et al., 1999; Tanida et al., 1999; Kabeya et al., 2000).

In the present study, we identified 25 Apg orthologs belonging to the model plant Arabidopsis. Both the functional domains and the amino acid residues essential for yeast autophagy are well conserved in the corresponding AtAPG proteins, suggesting that the Apg system functions in a similar manner in plants as it does in yeast and mammalian cells. To examine the physiological role of autophagy in plants, we searched for T-DNA insertional mutant plants in *AtAPG* genes and identified an *AtAPG9*-insertional mutant plant that we dubbed *atapg9-1*. *atapg9-1* plants were capable of completing the normal life cycle but displayed early senescence, a phenotype that was exaggerated under nutrient-deficient conditions. This is the first report, to our knowledge, to describe the phenotype of an *APG* plant mutant.

RESULTS

Identification of Arabidopsis *AtAPG* Genes

To identify *APG* genes (essential for autophagy) in Arabidopsis, we searched the Arabidopsis expressed sequence tag (EST) and genomic databases using BLAST. The search successfully identified 25 genes that encode proteins with significant homology to 12 of the 15 Apg proteins. Orthologs of the remaining three Apg genes (Apg14, Apg16, and Apg17) have thus far not been found in other organisms, suggesting that they are not well conserved. At the present time, 23 of the 25 corresponding EST or cDNA clones have been deposited in the National Center for Biotechnology Information/EMBL/DNA Data Bank of Japan database (with the exception of *AtAPG2* and *AtAPG10*). However, ESTs corresponding to *AtAPG2* and *AtAPG10* were found in other plant species as well. We then cloned most of the cDNAs by reverse transcriptase (RT)-PCR and 5′/3′-RACE and determined their intron/exon boundaries by comparing genomic sequences with the corresponding cDNAs. In many cases, the predicted coding sequences annotated in the database were not correct.

Figure 1 shows a diagram comparing yeast Apg proteins and Arabidopsis AtAPG proteins. Not only do all of the AtAPG proteins show significant homology to yeast Apg genes, but the functional domains and essential amino acid sequences of the yeast Apg genes are also well conserved as follows. Three Arabidopsis genes (*AtAPG1a*, *AtAPG1b*, and *AtAPG1c*) were assigned to Apg1p, a protein kinase whose activity is essential for autophagy (Matsuura et al., 1997). All AtAPG1 proteins contain an N-terminal kinase domain with a high degree of similarity to Apg1p, in addition to a less homologous region in the C-terminal half. Apg13p, the regulatory subunit of Apg1 kinase (Funakoshi et al., 1997; Kamada et al., 2000), displayed overall homology with AtAPG13a and AtAPG13b.

In the yeast Apg12 conjugation system, the C-terminal Gly of Apg12p is conjugated to a Lys residue

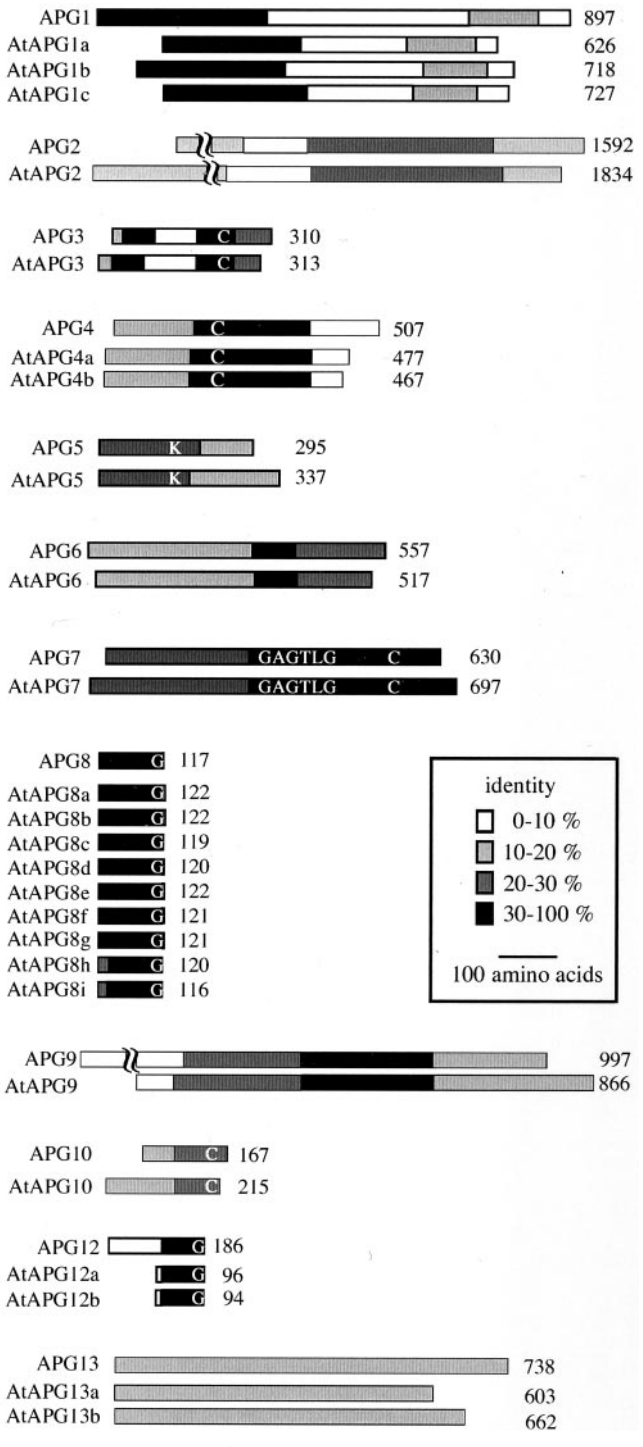

Figure 1. Comparison of yeast Apg proteins and Arabidopsis AtAPG proteins. The shading indicates the degree of identity between each homologous region. Each protein was aligned based on the CLUSTAL V method using DNASTAR. Conserved amino acid residues important for proper Apg function are indicated by letters. The numbers indicate the amino acid length of each protein. Accession numbers for the *AtAPG* sequences are: *AtAPG1a*, AAK59554; *AtAPG3*, AB073170; *AtAPG4a*, AB073171; *AtAPG4b*, AB073172; *AtAPG5*, AI997825; *AtAPG6*, AAK62668; *AtAPG7*, AB073173; *AtAPG8a*, AB073175; *AtAPG8b*, AB073176; *AtAPG8c*, AB073177; *AtAPG8d*, AB073178; *AtAPG8e*, AB073179; *AtAPG8f*, AB073180; *AtAPG8g*, AB073181; *AtAPG8h*, AB073182; *AtAPG8i*, AB073183; *AtAPG9*, AB073174; *AtAPG12a*, AB073184; and *AtAPG12b*, AB073185. The rest of the AtAPG protein sequences are predicted based upon genome sequence. Accession numbers for the corresponding BAC clones are: *AtAPG1b*, AL132960; *AtAPG1c*, AC007661; *AtAPG2*, AP000419; *AtAPG10*, AC009853; *AtAPG13a*, AL132964; and *AtAPG13b*, AB026654.

on Apg5p via an isopeptide bond in a ubiquitination-like manner. This conjugation reaction is mediated by Apg7p, a ubiquitin-activating enzyme (E1)-like protein, and by Apg10p, a ubiquitin-conjugating enzyme (E2)-like protein (Mizushima et al., 1998a; Shintani et al., 1999; Tanida et al., 1999). Lys-149 of Apg5p, essential for Apg5/Apg12 conjugation, corresponds to Lys-128 of AtAPG5. Both the ATP-binding motif Gly-X-Gly-X-X-Gly and Cys-507 of Apg7p, which are essential for E1-like activity, are conserved in AtAPG7. Cys-133 of Apg10p, at the active site of Apg10p, corresponds to Cys-178 of AtAPG10. The C-terminal Gly of Apg12p, through which Apg12p is covalently attached to Apg5p, is conserved in both AtAPG12a and AtAPG12b.

In the Apg8 lipidation system, another ubiquitin-like system essential for autophagy, the Apg4p protease removes the carboxy-terminal Arg of Apg8p and leaves a Gly residue at the C terminus of Apg8p. Apg8p is then activated by Apg7p and is subsequently attached to Apg3p, another E2-like enzyme, after which the C-terminal Gly of Apg8p is conjugated to phosphatidylethanolamine by an amide bond (Ichimura et al., 2000; Kirisako et al., 2000). Comparison of these four Apg8 system proteins (Apg3p, -4p, -7p, and -8p) with their Arabidopsis counterparts again reveals a considerable number of conserved essential residues. Cys-234 of Apg3p corresponds to Cys-258 of AtAPG3, which serves as an active site to catalyze the E2-like reaction in the Apg8 system. Cys-159 of Apg4p, which functions as the catalytically active amino acid for processing of Apg8, aligns with Cys-170 of AtAPG4a and Cys-173 of AtAPG4b.

Nine homologs of Apg8 were found in the Arabidopsis genome. All of them display an extremely high degree of identity (approximately 70%) with Apg8p and contain Gly at their carboxyl end. Two of nine orthologs, AtAPG8h and AtAPG8i, do not possess an extra amino acid tail downstream of the conserved Gly. The biological meaning of this gene duplication is still unclear. It may indicate the existence of a number of subtly different autophagy pathways in plants that may have their own organ-specific function. In fact, immunoblotting of AtAPG8 revealed an organ-specific banding pattern (H. Hanaoka, T. Noda, and Y. Ohsumi, unpublished data). Further characterization of each AtAPG8 molecule will hopefully yield answers to this interesting question.

We performed complementation tests with AtAPG3, -4a, -4b, -7, -9, -12a, and -12b using the corresponding yeast *apg* mutants. In yeast, amino-

peptidase I (API) is synthesized in the cytosol as a precursor enzyme, prAPI (61 kD). Under starvation conditions, prAPI is transported to the vacuole via autophagy where it is processed to mature API (mAPI, 50 kD; Klionsky and Ohsumi, 1999). By the test of API maturation, we found that AtAPG4a and AtAPG4b could complement the autophagic defect of the *apg4* mutant (Fig. 2). Fruitfly (*Drosophila melanogaster*) *Apg4* homolog was also recently reported to be able to complement yeast *apg4* mutation (Thumm and Kadowaki, 2001). AtAPG4a and -4b are the second Apg orthologs from multicellular organisms that could complement the biological function of yeast Apg proteins. Other *AtAPG* genes did not complement the autophagic defect of corresponding yeast *apg* mutant (data not shown), which is also the case in the mammalian Apg orthologs tested so far. Thus, this genome-wide scan has revealed a remarkable level of conservation in this gene family between yeast and higher plants.

Identification of *atapg9-1*, a T-DNA Insertional Mutant

To investigate the physiological role of autophagy in higher plants, we screened the Kazusa DNA Research Institute (Chiba, Japan) T-DNA insertion lines for *AtAPG* mutants. For analysis of autophagy-defective plant mutants, mutants in *AtAPG* genes that exist as a single copy in the genome were desired. With these criteria, an Arabidopsis line carrying the T-DNA insertion within the *AtAPG9* gene was identified.

The *AtAPG9* cDNA contains a putative open reading frame encoding for a hydrophobic protein of 866 amino acids. Figure 3 shows the amino acid alignment of the Apg9 orthologs found in Arabidopsis and other organisms. We noticed that there is a highly conserved region corresponding to AtAPG9 Trp-206-Gly-549. Yeast Apg9p was suggested to be an integral membrane protein (Noda et al., 2000), and hydrophilicity analysis of the APG9 orthologs shows that the conserved region corresponds well to the multimembrane-spanning domains of the middle region (data not shown). On the other hand, the NH_2- and COOH-terminal hydrophilic domains are somewhat divergent between the species. Based on the similarity of the predicted secondary structure, AtAPG9 is likely to be counterpart of yeast Apg9p.

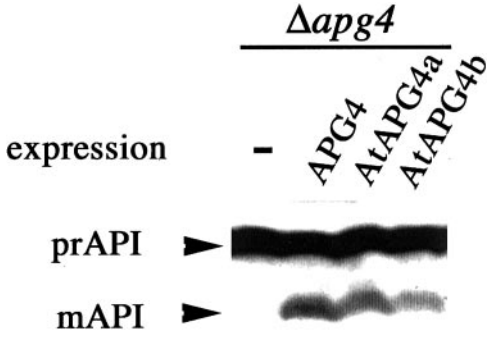

Figure 2. Complementation of yeast *apg4* mutants by AtApg4. Protein extracts from yeast Δ*apg4* mutant cells or those expressing yeast *APG4*, Arabidopsis AtAPG4a, or AtAPG4b were analyzed by immunoblot using antiserum against API. The positions of precursor and mature API are indicated.

Sequencing of the genomic PCR products carrying the T-DNA-genome junction revealed that the T-DNA was inserted within the third intron of *AtAPG9* and that the 3′ half of *AtAPG9* was lost and replaced by the T-DNA (Fig. 4A). The segregation pattern of antibiotic resistance indicated that this line carries a single-T-DNA insertion, an assumption that was confirmed by Southern-blot analysis using internal sequence of the T-DNA insertion as a probe (data not shown). We designated this line *atapg9-1*. The disruption of the *AtAPG9* gene by T-DNA insertion in *atapg9-1* was further confirmed by Southern-blot analysis using *AtAPG9* as a probe (Fig. 4B). The band pattern of *atapg9-1* completely differed from that of wild type. A single-hybridization-band pattern for each of the restriction enzymes tested indicates that *AtAPG9* is a single-copy gene in the Arabidopsis ecotype Wassilewskija genome. Upon completion of the genome sequence project, the lack of other Apg9 ortholog in the Arabidopsis ecotype Columbia genome was confirmed. To investigate the organ where *AtAPG9* was expressed, we performed RT-PCR using organ-specific RNA samples. The AtAPG9 transcript was detected in all tested wild-type organs: leaf, stem, flower, and root (Fig. 4C). Then we prepared protein samples from plant aerial parts and attempted to see the expression of AtAPG9 by western-blot analysis. The antibody raised against recombinant AtAPG9 recognized a band of 47 kD, which is much smaller than its predicted size in wild type, but not in the *atapg9-1* (Fig. 4D). The antibody recognized a band at the predicted size (99 kD) in yeast lysate depending on *AtAPG9* expression (Fig. 4E), so AtAPG9 protein may be prone to degradation during sample preparation. After three successive backcrosses to the wild type, the homozygous *atapg9-1* plants were propagated for further study.

Chlorosis Was Accelerated in *atapg9-1* Plants under Carbon Starvation

We observed the phenotype of *atapg9-1* under nutrient-deficient conditions. As assurance that our experiment results were the direct effect of null mutation of the *AtAPG9* gene, we transformed *atapg9-1* plants with wild-type *AtAPG9*, including its own promoter. No *AtAPG9* transcript was detected by RT-PCR in the homozygous *atapg9-1* plants, and the expression of *AtAPG9* was restored in mutant plants containing the wild-type *AtAPG9* transgene (Fig. 5A). First, growth under carbon starvation was observed. For carbon starvation, 7-d-old seedlings grown on

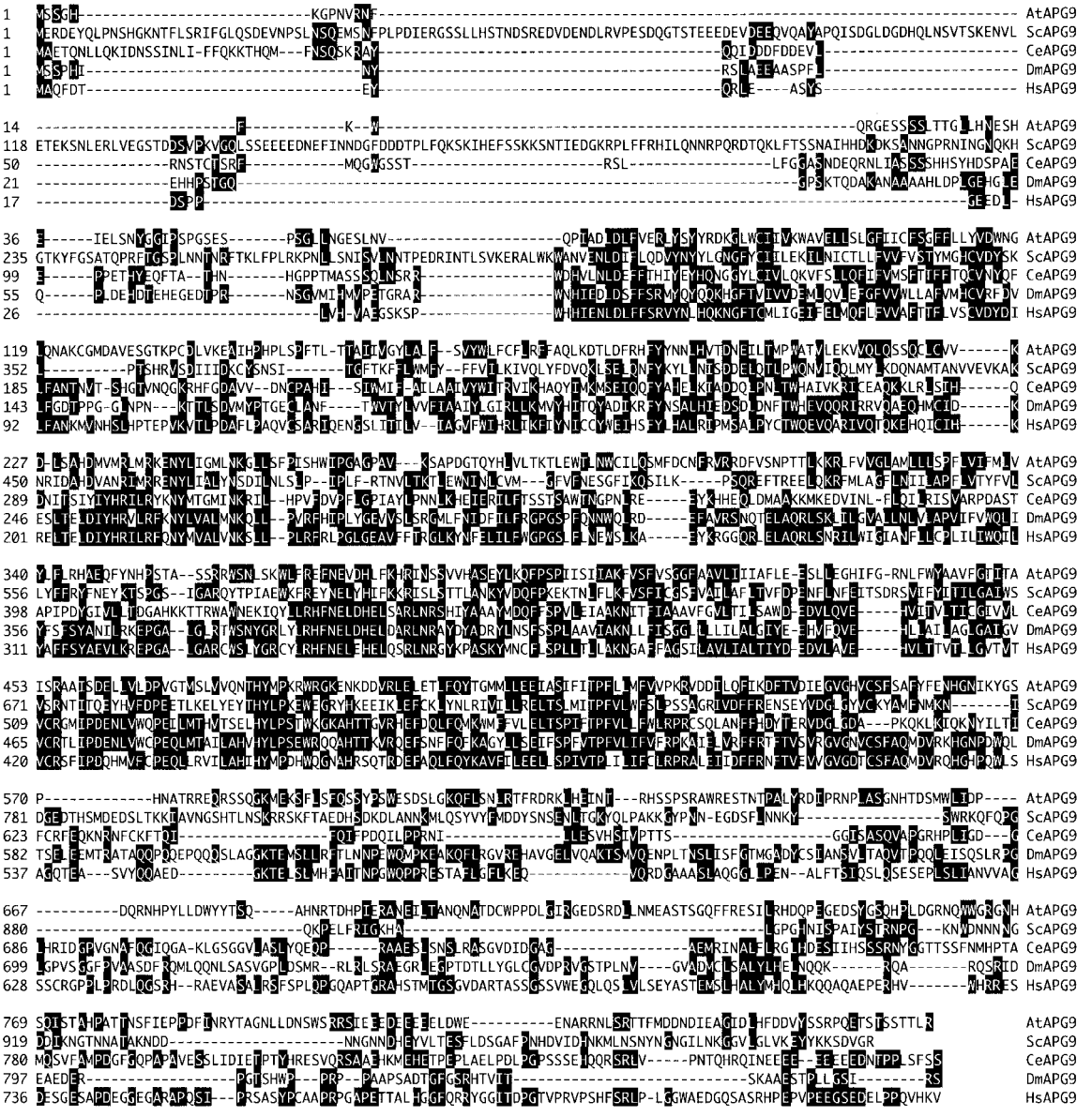

Figure 3. Amino acid alignment of AtAPG9 and its orthologs. Each protein was aligned by the CLUSTAL V method using DNASTAR. Residues that match the consensus are shaded in black. At, Arabidopsis; Sc, yeast; Ce, *Caenorhabditis elegans*; Dm, fruitfly; and Hs, human (*Homo sapiens*).

rockwool with 16-h-light/8-h-dark cycles were transferred to 24-h dark conditions. Figure 5B shows a photograph of the plant after 8 d of carbon starvation. The *atapg9-1* cotyledons turned yellow, whereas those of the wild-type plants retained a pale green color. The chlorophyll content was measured after transfer to the dark condition (Fig. 5C). The amount of chlorophyll per fresh weight was similar in both wild-type and *atapg9-1* plants at d 0, implying that chlorophyll synthesis is not affected by the mutation. In wild-type plants, the chlorophyll content started to decrease, and at d 10, it was one-half of its starting level. However, the decrease proceeded faster in *atapg9-1* plants. This phenotype was restored by complementation with wild-type *AtAPG9*, indicating that AtAPG9 functions in cell survival under carbon-starvation conditions.

Under Nitrogen Starvation, Chlorosis Was Accelerated and Seed Production Was Affected in *atapg9-1* Plants

Growth under nitrogen-starvation conditions was also analyzed. For nitrogen starvation, 10-d-old seedlings grown in nutrient medium (7 mM nitrate) were transferred to nitrogen-depleted medium (0 mM nitrate). Nitrate was the sole nitrogen source of the culture media used in this study. After 14 d of nitro-

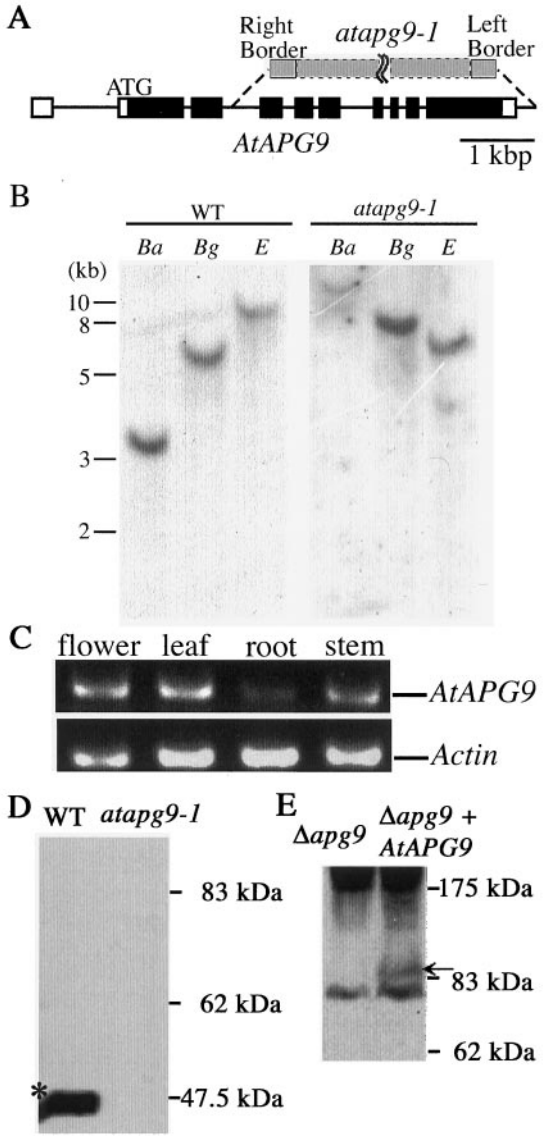

Figure 4. Identification of the mutant *atapg9-1*. A, Genomic structure of the *AtAPG9* gene. Lines indicate introns and boxes indicate exons; white boxes, untranslated regions; and black boxes, translated regions. The T-DNA insertion site in the *atapg9-1* allele is indicated by the gray box. B, Southern-blot analysis of the *AtAPG9* gene. Arabidopsis genomic DNA from wild-type (WT) and *atapg9-1* mutant plants was digested with *Bam*HI (Ba), *Bgl*II (Bg), or *Eco*RV (E), and the blot was hybridized with an *AtAPG9* probe. C, The expression of *AtAPG9* in various organs. Total RNA was isolated from flowers, leaves, stems, and roots of wild-type plants grown hydroponically for 1 month. RT-PCR was performed using gene-specific primers for *AtAPG9* and for actin *ACT2* gene. After agarose electrophoresis, the gel was stained with ethidium bromide. D, Immunoblotting of AtAPG9 in plant lysates. Total plant lysates prepared from wild-type plants (WT) and *atapg9-1* mutant plants were centrifuged at 100,000*g* for 1 h, and the pellets were subjected to the immunoblot using anti-AtAPG9. Possible degradation product of AtAPG9 is marked by the asterisk. E, Immunoblotting of AtAPG9 in yeast lysates. Yeast total lysates were prepared from yeast Δ*apg9* cells or Δ*apg9* cells expressing AtAPG9 as described in "Materials and Methods." AtAPG9 (predicted molecular mass = 99 kD) is indicated by the arrow.

gen starvation, chlorosis was induced earlier in *atapg9-1* plants than wild-type plants (Fig. 5D). Time-course analysis indicated that the rate of chlorophyll degradation in *atapg9-1* first and second rosette leaves was 20% higher than in wild-type leaves (Fig. 5E).

The seed production of *atapg9-1* was examined under nitrogen-starvation conditions. As a result, *atapg9-1* plants did not produce as many seeds as wild-type plants under nitrogen-starvation conditions. As shown in Figure 6A, wild-type plants could bear mature silique even in fifth and sixth flowers, whereas most of *atapg9-1* plants could not. Most *atapg9-1* plants produced only four flowers, thus, the average number of mature silique per mutant plant was less than that of wild type (Fig. 6B). Because Arabidopsis is known to form a certain number of seeds before the meristem arrest; seeds per silique may, therefore, increase in *atapg9-1* to produce the same number of seeds as wild-type plants. So, we checked the number of seeds per plant. The number of seeds produced in *atapg9-1* plants (19.5 ± 4.8) was less than that of wild-type plants (25.8 ± 5.8). Student's *t* test or Mann-Whitney's *u* test indicated that the number of seeds in *atapg9-1* was significantly different from that of wild type ($P < 0.05$). These phenotypes were restored in mutant plants expressing transgenic wild-type *AtAPG9*. *atapg9-1* showed the decrease both in the number of siliques and the number of seeds per plant under the nitrogen-starved condition.

Bolting and Natural Leaf Senescence Were Accelerated in *atapg9-1*

With a supply of typical nutrient solution, *atapg9-1* did not exhibit significant mutant phenotypes in germination, cotyledon development, elongation of the root system and the inflorescence stem, and seed production. However, bolting of *atapg9-1* was accelerated (Fig. 7A). In four independent experiments, *atapg9-1* always began bolting 2 or 3 d earlier than wild-type plants (Fig. 7B). The average rosette leaf number at the time of bolting was reduced in *atapg9-1* (9.2 ± 0.9) compared with wild type (11.4 ± 1.0). This early flowering phenotype was rescued by expressing transgenic wild-type *AtAPG9* in *atapg9-1* plants.

Rosette leaves of *atapg9-1* plants senesced earlier than those of wild-type plants (Fig. 7C). *atapg9-1* rosette leaves were morphologically indistinguishable from their wild-type counterparts at 17 d after germination, but the edges of these leaves started to turn yellow in *atapg9-1* plants at d 35, whereas wild-type leaves were still green. Natural senescence in *atapg9-1* plants progressed in an orderly fashion from the old lower leaves to the young upper leaves as in wild-type plants.

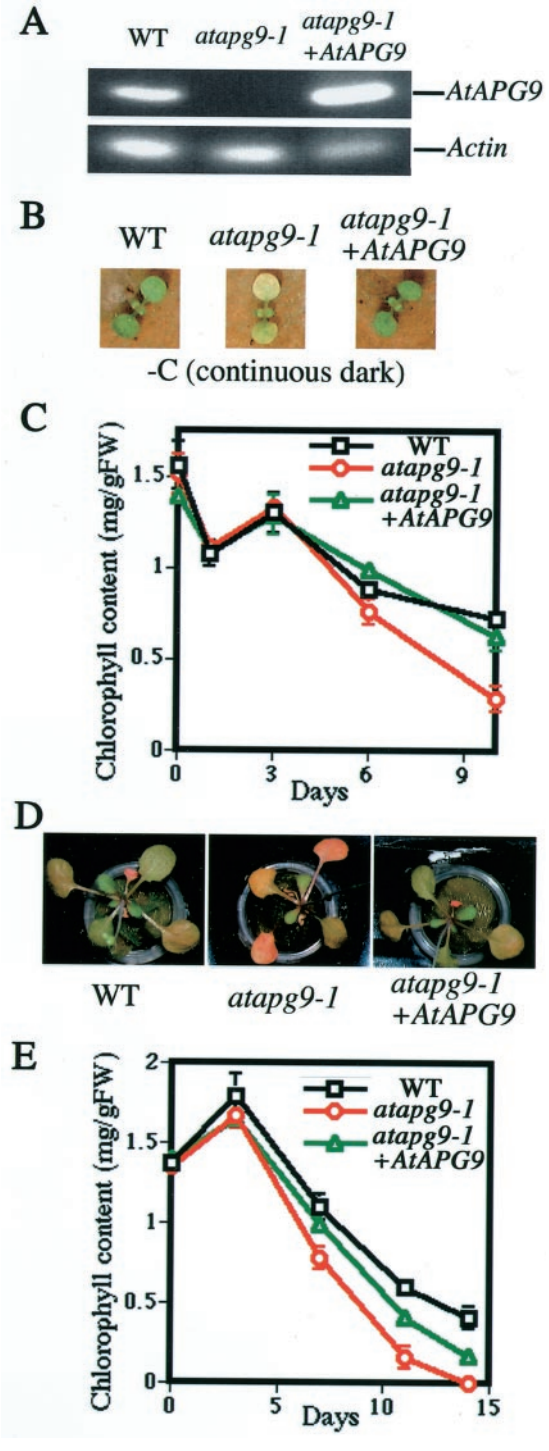

Figure 5. AtAPG9 expression in *atapg9-1* suppresses carbon or nitrogen starvation-induced chlorosis. A, RT-PCR of *AtAPG9* gene. Total RNA was isolated from leaves of wild type, *atapg9-1*, and *atapg9-1* transformed with the *AtAPG9* gene. RT-PCR was performed using gene-specific primers for *AtAPG9* and for actin *ACT2* gene. After the agarose electrophoresis, the gel was stained with ethidium bromide. B, Top view of 15-d-old carbon-starved plants. Plants were photographed after 8 d of carbon starvation. C, Time-course analysis of chlorophyll content. Plants were grown for 7 d with a light cycle of 16 h light/8 h dark, after which they were maintained in the dark. Chlorophyll was extracted from two cotyledons at the day indicated after transfer to continuous dark conditions. D, Top view of 24-d-old nitrogen-starved plants. Plants were grown with nutrient medium containing 7 mM nitrate for 10 d and then transferred to nitrogen-depleted (0 mM nitrate) medium and grown hydroponically for 14 d. E, Time-course analysis of chlorophyll content. Chlorophyll was extracted from the first and second rosette leaves at the day indicated after induction of nitrogen starvation. All measurements were made on at least three individual plants.

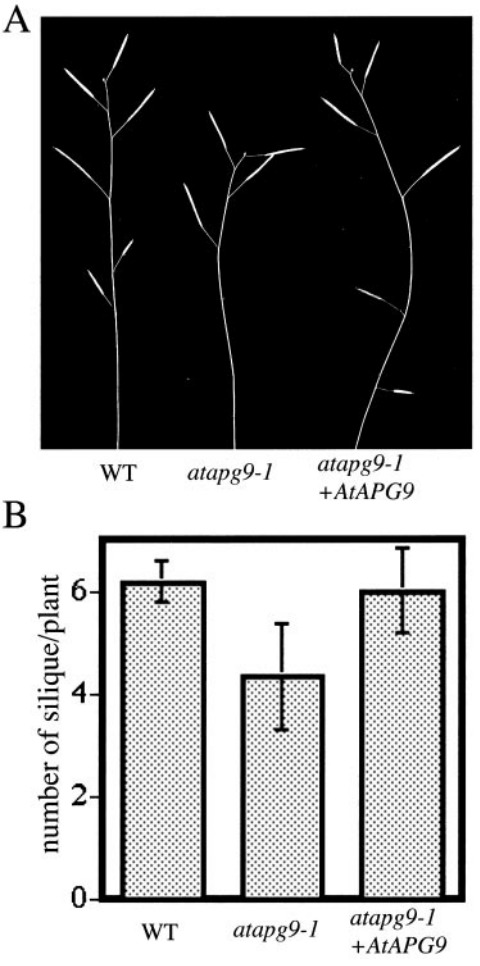

Figure 6. AtAPG9 deficiency impairs efficient seed production under nitrogen-starvation conditions. A, Representative 2-month-old plants grown hydroponically under nitrogen-starvation conditions. B, Number of siliques produced per plant grown under nitrogen-starvation conditions for 2 months. All measurements were made on at least four individual plants.

Characterization of *atapg9-1* during Artificially Induced Leaf Senescence

To characterize the leaf senescence more precisely, we employed the experimental system of artificially induced senescence. The third and fourth leaves of 3-week-old plants were detached and floated on water under dark condition. As found in attached leaf, leaf senescence was also accelerated in *atapg9-1* leaves (Fig. 8A).

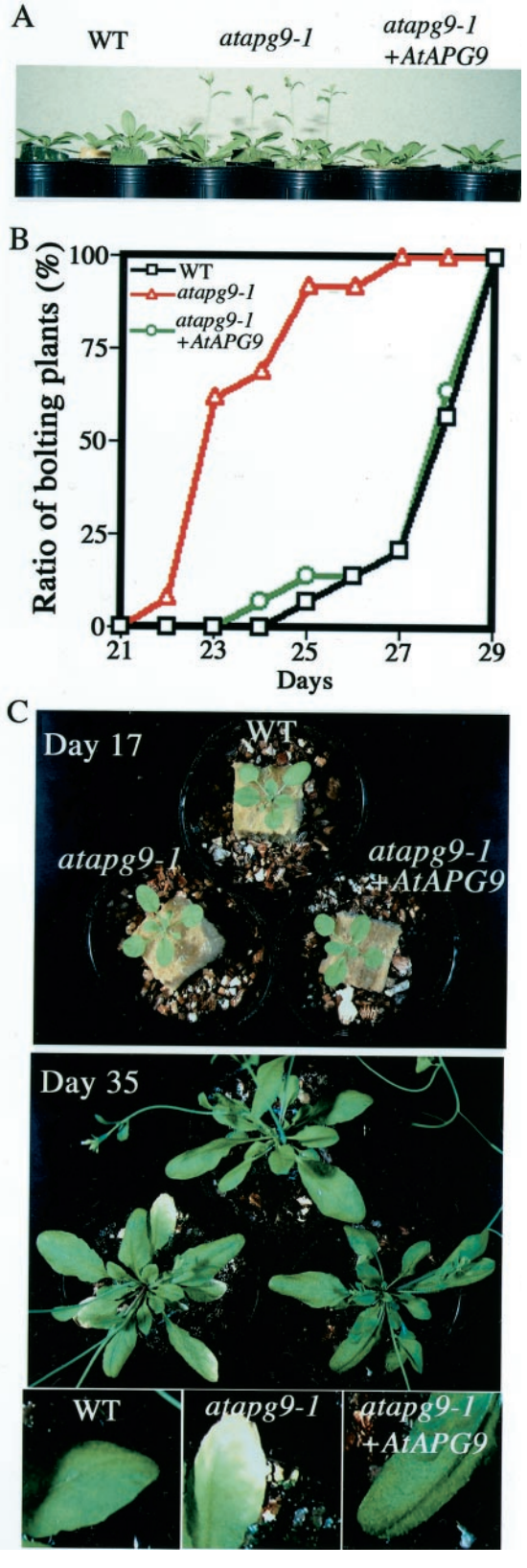

Figure 7. The phenotypes of *atapg9-1* under normal condition. A, Side view of 26-d-old plants. Wild-type and *atapg9-1* plants were grown at 22°C with a 16-h-light/8-h-dark cycle supplied with standard nutrient solution. B, Time-course analysis of bolting. The number of plants containing at least one primary inflorescence stem longer than 5 mm was counted daily. All measurements were made on at least 13 individual plants. C, Natural leaf senescence. Wild type, *atapg9-1*, and *atapg9-1* transformed with wild-type *AtAPG9* gene were grown under standard conditions and photographed on d 17 and 35 after germination. Magnified views were also shown.

To explore the cause of the difference, the total protein amount was measured at first (Fig. 8B). During initial the 48 h, total protein level was mostly kept constant both in wild type and *atapg9-1*. We also obtained a similar result in yeast. Neither wild-type nor *apg* mutant yeast cell decreased the total protein amount during starvation, which induced autophagy (J. Onodera and Y. Ohsumi, unpublished data). We interpreted this phenomena as the reuse of the degradation product and the maintenance of the net protein amount. However, *atapg9-1* showed less protein at 96 h, consistent with its early senescence.

We checked the expression of commonly known senescence-associated genes during the artificially induced senescence by semiquantitative RT-PCR analysis (Shimizu et al., 2001). The *SEN1* is induced only after 1 d in darkness, and *YSL4* is induced after a longer period of dark treatment (more than 48 h; Fig. 8C; Oh et al., 1996; Yoshida et al., 2001). In *atapg9-1*, significant expression of both genes was observed before dark incubation. This result implies that *atapg9-1* exists as senescence status before induction of senescence in this experimental condition.

Next, vacuolar morphology during leaf senescence was compared using green fluorescent protein (GFP) fused γ-tonoplast intrinsic protein (TIP) as a vacuolar membrane marker. The transgenic lines expressing γ-TIP-GFP were made both of wild-type and *atapg9-1* background. Under normal growth condition, vacuoles of root, stem, and leaf cells of *atapg9-1* exhibited indistinguishable morphology from wild type (data not shown). Sometimes many bright spherical structures were observed in wild-type detached leaves in this experimental condition (Fig. 8D). Judging from their morphology and brightness, they were assumed to be the structure called a bulb that defines a subregion in the continuous vacuolar membrane (Saito et al., 2002). These structures were also observed in *atapg9-1* background. Further detailed analysis on this structure must be required to unveil the vacuolar membrane dynamics during senescence.

DISCUSSION

Here, we report the characterization of the first (to our knowledge) T-DNA insertional plant mutant of an autophagy-related gene. Of the total 15 *APG* genes that encode proteins necessary for yeast autophagy, 12 of them were found to have at least one homologous partner in Arabidopsis (Fig. 1). Because the functional domains of the resulting AtAPG proteins are well-conserved between yeast and plants, it

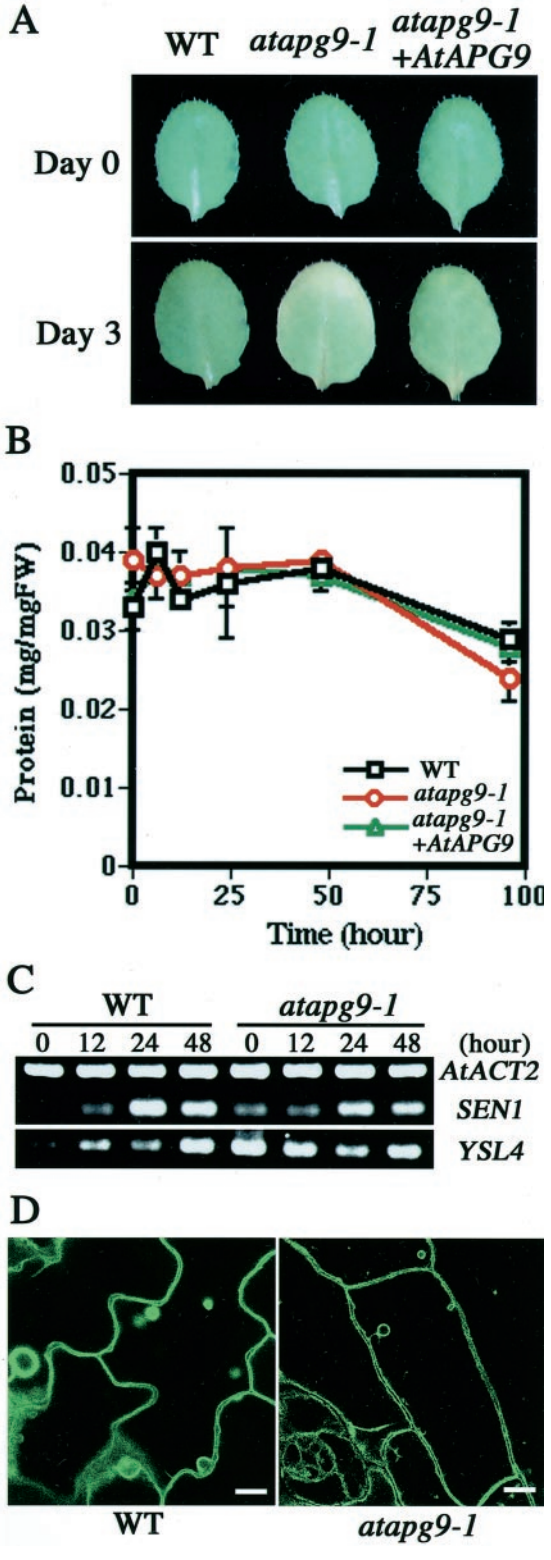

Figure 8. The phenotypes during artificially induced senescence. The third or fourth rosette leaves of 3-week-old plants were detached and floated on water at 22°C in the dark. A, Top view of detached leaves. The leaves were photographed at d 0 and after 3 d of incubation. B, Changes in protein content. Protein was extracted from the detached rosette leaves at the time indicated. All measurements were made on at least three individual plants. C, Expression of senescence-inducible genes. Total RNA (10 μg) isolated from wild type or *atapg9-1* were isolated at the time indicated. Semiquantitative RT-PCR was performed using gene-specific primers for *SEN1*, *YSL4*, and actin *ACT2* gene. After the agarose electrophoresis, the gel was stained with ethidium bromide. D, Vacuolar morphology of epidermal cells in detached rosette leaves. Detached rosette leaves of wild-type or mutant plants expressing γ-TIP-GFP were observed after 12 h of incubation in water. Scale bar = 10 μm.

seems likely that their biological functions would be equally well-conserved. We confirmed that both *AtAPG4a* and *AtAPG4b* can complement the autophagic defect of the yeast *apg4* mutation (Fig. 2). Based on these facts, it is reasonable to assume that the AtAPG proteins are involved in autophagy in plant cells. This assumption has been proven in mammalian cells, because several mammalian APG proteins have been shown to be essential for autophagy (Liang et al., 1999; Mizushima et al., 2001) and to act via a molecular mechanism quite similar to that of yeast (Mizushima et al., 1998b; Kabeya et al., 2000; Tanida et al., 2001).

Because *AtAPG9* is the only ortholog of yeast *APG9* in the Arabidopsis genome, its T-DNA insertional mutant, *atapg9-1*, would be expected to be an autophagy-deficient plant. Another group recently isolated an *AtAPG7* T-DNA insertional mutant plant, *atapg7-1*. Similar phenotypes to that of *atapg9-1* were observed in *atapg7-1* (J.H. Doelling and R.D. Vierstra, personal communication). This strongly supports the idea that both AtAPG7 and AtAPG9 are essential components of the plant autophagy machinery and that their phenotypes are the result of defects in autophagy.

At early growth stages under nutrient conditions, a significant mutant phenotype was not observed in the *atapg9-1* mutant. However, nutrient starvation made it easy to distinguish *atapg9-1* from wild-type plants. *atapg9-1* plants began to die earlier than wild-type plants under nitrogen or carbon starvation (Fig. 5). Several preceding studies have indicated that autophagy is induced by nutrient starvation in plant cells (Aubert et al., 1996; Moriyasu and Ohsumi, 1996). Therefore, the starvation-induced phenotype of *atapg9-1* must stem from a defect in autophagy. Similar phenotypes were also observed in yeast (Tsukada and Ohsumi, 1993). During starvation, wild-type yeast cells maintain viability, whereas *apg* mutant cells begin to die. The reason why autophagy-deficient yeast cells die is still unknown, although one possible explanation is that cytoplasmic constituents degraded by autophagy are meant to be used as a nutrient resource and are necessary for maintaining cell viability during starvation.

In addition to the starvation-induced phenotype, *atapg9-1* displayed early flowering and leaf senescence under nutrient conditions (Fig. 7). This result suggests that autophagy occurs in plants not only during starvation. Autophagy seems to be genetically

programmed to occur before or during senescence regardless of nutrient status, because senescence-related genes were induced in spite of induction of senescence in *atapg9-1* (Fig. 8C).

If autophagy contributes to the cellular degradation process during leaf senescence, then why is the leaf senescence process not inhibited in the *atapg9-1* plant, and why does it not remain green? Degradative processes other than autophagy occur during senescence, such as degradation of chloroplast proteins by chloroplast intrinsic proteases (Bushnell et al., 1993) and the collapse of the vacuolar membrane (Inada et al., 1998). In addition, in the senescing soybean leaf, protrusion of numerous plastoglobules from chloroplasts was observed (Guiamet et al., 1999). These globules secreted from the chloroplast were suggested to carry the photosynthetic components to the cytoplasm or the vacuoles to be degraded. Park et al. (1999) reported a similar phenomenon, namely transfer of proteins from chloroplasts to vacuoles for degradation in *Chlamydomonas reinhardtii*. Leaf senescence in *atapg9-1* may depend on these other degradative processes. Ono et al. (1995) reported that two different phases of degradation occur in wheat (*Triticum aestivum*) natural leaf senescence. About 20% of chloroplasts were lost during the first phase, and the remainders were rapidly degraded during the second phase. Thus, plant cells will orchestrate the regulation of several different degradation mechanisms during senescence to accomplish efficient nutrient relocalization. It is well known that plants relocate nutrients from old to young tissues. Autophagy may help to maintain viability during senescence/starvation as seen in yeast, and without it, plant cells may degrade themselves by other mechanisms and die. Because of acceleration of cell death, *atapg9-1* may not be able to relocate nutrients efficiently, a process that may require ordered cell death dependent on autophagy. Early senescence (Fig. 7) and the reduced seed sets (Fig. 6) in *atapg9-1* must be caused by the less efficient use of available nutrients in *atapg9-1*. The effect of nutrition on flowering time in Arabidopsis has not been analyzed in detail. Effects of sugar on floral transition in Arabidopsis were recently investigated precisely (Ohto et al., 2001). More work of this type would be required to understand the effect of autophagy on the floral transition.

This study provided the first hints, to our knowledge, as to when and where autophagy occurs in Arabidopsis. From the time-course analysis of chlorophyll contents, *atapg9-1* plants start to show an aberrant phenotype at roughly d 3 after initiation of starvation. This suggests that autophagy was induced within 3 d after transfer, which is in agreement with results from studies on autophagy induction in cultured cells or in whole plants during starvation (Moriyasu and Ohsumi, 1996; Brouquisse et al., 1998). *AtAPG9* was expressed in all tested tissues, and thus, autophagy may occur in all of these tissues, but dramatic induction of *AtAPG9* transcription was not observed during starvation of Arabidopsis suspension-cultured cells, which is the case also in yeast cells (Noda et al., 2000; H. Hanaoka, T. Noda, and Y. Ohsumi, unpublished data). Apg9p was shown to be localized to large perivacuolar punctate structures, which are possibly precursor structures of the autophagosome, and is required for functional localization of several Apg proteins (Wang et al., 2001; Noda et al., 2000; Suzuki et al., 2001). AtAPG9 was predicted to be an integral membrane protein, as is its ortholog in yeast, and was expected to play an important role in autophagosome formation. Because of its tendency to be degraded after isolation, however, biochemical studies on AtAPG9 have not progressed thus far. We are currently working to solve this problem. Further study of this and other AtAPG proteins promises to yield a better understanding of autophagy in plants, both at the molecular and organismal level. The morphological analysis of autophagy in Arabidopsis has not been reported yet. Some of AtAPG proteins are good candidates as the marker of autophagosome, they must be powerful tool for further ultrastructural analysis of autophagy in Arabidopsis. We are at the beginning of an exciting new stage in the study of plant autophagy.

MATERIALS AND METHODS

Plant Material and Culture Conditions

All experiments were performed using Arabidopsis ecotype Wassilewskija, except for isolation of the *AtAPG9* cDNA clone, which was from Arabidopsis ecotype Columbia. The plants were grown on rockwool using vermiculite as soil at 22°C with 16-h-light/8-h-dark cycles, using hydroponic media as nutrient solution. As an alternative, the hydroponic culture was carried out as described in Hirai et al. (1995). In brief, hydroponic cultures were initiated by putting 10-d-old seedlings on floats in hydroponic media. The media were aerated and changed twice per week. The hydroponic media contained 1.5 mM NaH_2PO_4, 0.26 mM Na_2HPO_4, 1.5 mM $MgSO_4$, 2.0 mM $Ca(NO_3)_2$, 3.0 mM KNO_3, 30 μM H_3BO_3, 8.7 μM NaFe-EDTA, 10.3 μM $MnCl_2$, 1.0 μM $ZnCl_2$, 1.0 μM $CuCl_2$, 130 nM $CoCl_2$, and 24 nM $(NH_4)_6Mo_7O_{24}$.

For carbon starvation, 7-d-old seedlings grown on rockwool were subjected to 24-h-dark conditions. For nitrogen starvation, 10-d-old seedlings grown on rockwool were transferred to nitrogen-depleted medium and grown hydroponically. A nitrogen-depleted medium was prepared by replacing KNO_3 and $Ca(NO_3)_2$ with KCl and $CaCl_2$, respectively.

Cloning of *AtAPG* Genes

Genes homologous to yeast (*Saccharomyces cerevisiae*) *APG* were searched for in the Arabidopsis ecotype Columbia EST and genomic databases using the BLAST program. *AtAPG* cDNA sequences were determined by various methods. RT-PCR was performed to amplify the predicted coding region for *AtAPG3*, *-4a*, *-4b*, *-7*, *-8a*, *-8b*, *-8c*, *-8d*, *-8e*, *-8f*, *-8g*, *-8h*, *-8i*, *-9*, *-12a*, and *-12b*. Each cDNA was obtained from PCR products using the Marathon cDNA amplification kit (CLONTECH, Palo Alto, CA) and subcloned into pBluescript SK+ (Stratagene, La Jolla, CA). Each cDNA was then sequenced, and the sequences were deposited into DNA Data Bank of Japan/National Center for Biotechnology Information/EMBL. For *AtAPG1a*, *AtAPG5*, and *AtAPG6*, a cDNA sequence had previously been deposited by other groups. For *AtAPG1b*, *-1c*, *-2*, *-10*, *-13a*, and *-13b*, coding regions were predicted based on a comparison of the Arabidopsis genomic DNA sequence with

several APG orthologs from other organisms. A splicing site prediction program was also used.

Screening of T-DNA Insertion Lines

We used the T-DNA insertion-line screening system engineered at the Kazusa DNA Research Institute. The principles of the screening method have been previously described (McKinney et al., 1995). *AtAPG9*-specific primers used for screening were 5′-ATGAGCAGTGGGCATAAGGGTCCAAATG-3′ and 5′-TCACCGTAATGTGGTGCTTGATGTTG-3′. The T-DNA-specific primers were 5′-TAGATCCGAAACTATCAGTG-3′ and 5′-ATAACGCT-GCGGACATCTAC-3′. We used four combinations of primer sets, each consisting of a gene-specific primer and a T-DNA-specific primer. The position of the T-DNA insert was determined by sequencing the PCR products carrying the T-DNA-genome junctions.

Southern-Blot Analysis

Total genomic DNA isolated from wild-type and mutant Arabidopsis was digested with various restriction enzymes and subjected to Southern-blot analysis following standard protocols for the DIG system (Roche Diagnostics, Tokyo). Digoxigenin-labeled *AtAPG9* probes were hybridized to the membrane-bound DNA at 42°C in 5× SSC (20× SSC = 3 M NaCl and 0.3 M sodium citrate), 0.1% (w/v) *N*-lauroylsarcosine, 0.02% (w/v) SDS, 1% (w/v) blocking reagent, and 50% (v/v) formamide. Washing was performed at 68°C in 0.1× SSC and 0.1% (w/v) SDS, and the blots were analyzed for chemiluminescence.

Complementation Test of Yeast *apg* Mutants with *AtAPG* Genes

To express AtAPG proteins in yeast, each *AtAPG* gene was inserted under the GAP promoter of yeast expression vector pKT10 (Tanaka et al., 1990). Yeast strains were grown in standard rich medium (yeast peptone dextrose) or starvation medium as described previously (Noda et al., 2000). Yeast strains used in the complementation test were described previously (Kirisako et al., 2000).

Yeast whole-cell lysates were prepared by breaking the cells in 0.2 M NaOH and 1% (v/v) 2-mercaptoethanol. Then proteins were precipitated by addition of trichloroacetic acid; and after centrifugation, samples were washed with cold acetone, subjected to the 9% (w/v) polyacrylamide SDS-PAGE, and analyzed by immunoblotting using anti-API antibody as previously described (Noda et al., 2000).

Western Blotting of AtAPG9

Anti-AtAPG9 antibody against His-tagged AtAPG9 was prepared by immunization of rabbits and affinity purified. To produce His-tagged AtAPG9, the part of *AtAPG9* cDNA fragment encoding C-terminal 247 amino acids was prepared by *Hin*dIII digestion. This fragment was cloned into expression vector, pET28b (Novagen, Madison, WI) digested with *Hin*dIII. The resulting plasmid pHH20 was expressed in *Escherichia coli*, and His-tagged AtAPG9 recombinant protein was purified by Ni column.

Yeast whole-cell lysates were prepared in the same way as in "Complementation Test of Yeast *apg* Mutants with *AtAPG* Genes."

Plant protein samples were prepared as follows: 300 mg of plant aerial parts of was homogenized in 0.6 mL of extraction buffer (50 mM HEPES-KOH, pH 7.5, 10 mM KOAc, 1 mM EDTA, 0.4 M Suc, 1 mM dithiothreitol, 2 mM phenylmethylsulfonyl fluoride, and 5% (v/v) plant protease inhibitor cocktail (P-9599, Sigma, St. Louis). The lysate was centrifuged at 4°C, 1,000*g*, for 10 min. The pellet was discarded, and the supernatant was then ultracentrifuged at 4°C, 100,000*g*, for 1 h. The pellet was analyzed by SDS-PAGE, followed by immunoblotting.

RT-PCR Analysis of *AtAPG9* Expression

Total RNA was extracted from each samples using ISOGEN (Nippon Gene, Tokyo), and cDNA was generated using the ProSTAR RT-PCR kit (Stratagene) following the manufacturer's instructions. For PCR, *AtAPG9*-specific primers (5′-TTGGATCTTTTTGTCGAAAGGCTCTAC-3′ and 5′-AAAG-CTG-CAAACATGGCCTACACC-3′) and Arabidopsis *ACTIN2*-specific primers (5′-ATGAAGATTAAGGTCGTTGCACCACC-3′ and 5′-CTTATATTAACA-TTG-CAAAGAGTTTCAAGG-3′) were used. The PCR reaction for AtAPG9 consisted of 30 cycles of 94°C for 30 s, 56°C for 30 s, and 72°C for 90 s.

RT-PCR Analysis of *SEN1* and *YSL4* Expression during Artificially Induced Senescence

Total RNA was extracted from each samples using a CsCl step gradient (Chirgwin et al., 1979), and cDNA was generated using the ProSTAR RT-PCR kit (Stratagene) following the manufacturer's instructions. Ten micrograms of total RNA was used as templates. For PCR *SEN1*-specific primers (5′-ATCACGAATTGGAAACTGG-3′ and 5′-CTTTCCTCCATCGGAAG-3′) and *YSL4*-specific primers (5′-GCTCGCTGGTTTGACAG-3′ and 5′-TGGAGAAGCACTATAGAACC-3′) were used. The reaction for *SEN1* (30 cycles) and *YSL4* (28 cycles) consisted of 94°C for 30 s, 52°C for 30 s, and 72°C for 30 s. The number of the cycle was determined to ensure the PCR product was not saturated.

Analysis of Floral Transition Time

The plants were grown on rockwool using vermiculite as soil. Floral transition time was scored as the time at which the main inflorescence shoot had elongated to 5 mm.

Artificial Induction of Leaf Senescence

The third and the fourth rosette leaves of 3-week-old plants were detached and floated on deionized water in 12-well petri dishes, adaxial side up (Oh et al., 1996). Leaves were incubated at 22°C in the dark.

Protein Analysis during Artificially Induced Senescence

Proteins were extracted from frozen powdered material with the following extraction buffer: 50 mM Tris-HCl, pH 6.8, 2% (w/v) SDS, and 10% (v/v) glycerol. The lysate was boiled for 10 min and then centrifuged at 4°C, 15,000 rpm, for 10 min. The protein concentration of supernatant was then measured with the BCA (bichinchoninate) acid protein assay kit (Pierce, Rockford, IL) using bovine serum albumin as a standard.

Determination of Chlorophyll Content

Chlorophyll was extracted from fresh cotyledons or first and second rosette leaves with methanol at 4°C for 1 d. The extracts were subjected to spectrophotometric measurements at 625, 647, and 664 nm. Chlorophyll contents were calculated using a Moran equation (Moran, 1982).

Complementation Test of *atapg9-1*

The *AtAPG9* gene, including 3 kb upstream from the start codon, was amplified by PCR from genomic DNA using two sets of primers, 5′-ACCGCTCGAGTTTT-CAACTGGTTTCCTTC-3′ and 5′-GCGGATCCCAG-AGAAGCATATGATG-3′ or 5′-TTGGATCTTTTTGTCGAAAGGCTCTAC-3′ and 5′-AGTCGAGCTCACCG-TAATGTGGTGCTTGA-3′. The first amplified fragment, attained using the former set of primers, was cloned into pBluescript KS+ digested with *Eco*RV. The resulting plasmid pHH34 was digested with *Nde*I and *Sac*I and subsequently ligated with the second amplified fragment digested with *Nde*I/*Sac*I. Next, the *Xho*I-*Sac*I fragment was cloned into the binary vector pBI121Δ35S, a derivative of pBI121 (Hayashi et al., 2000). The resulting plasmid pHH38 was introduced into the *Agrobacterium tumefaciens* strain C58C1Rif^r, which was then used to transform the Arabidopsis *atapg9-1* homozygous mutant by the floral dip method (Clough and Bent, 1998). Transgenic plants were identified by kanamycin resistance. Seven T1 plants were selected, and the T2 generation was screened for 3:1 (resistant: non-resistant) segregation. Two of these plant lines showed 100% resistance to kanamycin in the T3 generation, and these were selected as homozygous plant lines. The homozygous T3 and T4 plants were used for the following physiological experiments.

Analysis of Vacuolar Morphology using γ-TIP-GFP

Plants were transformed with binary vector carrying γ-TIP-GFP (Saito et al., 2002) in the same way as complementation test of *atapg9-1*. The T3 homozygous plants were subjected to the microscopic observation. Adaxial epidermal cells of rosette leaves were observed using a fluorescence laser scanning confocal microscope (LSM510, Zeiss, Jena, Germany).

Software Programs

Amino acid sequence alignment was performed using the program Megalign (DNASTAR, Madison, WI). Hydrophilicity analysis was performed using Protean (DNASTAR).

Distribution of Materials

Upon request, all novel materials described in this publication will be made available in a timely manner for non-commercial research purposes, subject to the requisite permission from any third-party owners of all or parts of the material. Obtaining any permissions will be the responsibility of the requestor.

ACKNOWLEDGMENTS

We thank Dr. Richard D. Vierstra and Dr. Jed H. Doelling for sharing their results before publication. We thank Dr. Masaaki Ohto, Dr. Tomoo Shimada, Dr. Kenji Yamada, Dr. Gyung-Tae Kim, Dr. Chieko Saito, and Dr. Akihiko Nakano for kindly providing plant materials, plasmids, and helpful technical instructions. We also thank Dr. Yuji Moriyasu, Dr. Takashi Okamoto, and Kiminori Toyooka for their helpful comments.

Received November 20, 2001; returned for revision February 7, 2002; accepted April 15, 2002.

LITERATURE CITED

Aubert S, Gout E, Bligny R, Marty-Mazars D, Barrieu F, Alabouvette J, Marty F, Douce R (1996) Ultrastructural and biochemical characterization of autophagy in higher plant cells subjected to carbon deprivation: control by the supply of mitochondria with respiratory substrates. J Cell Biol **133:** 1251–1263

Brouquisse R, Gaudillere JP, Raymond P (1998) Induction of a carbon-starvation-related proteolysis in whole maize plants submitted to light/dark cycles and to extended darkness. Plant Physiol **117:** 1281–1291

Bushnell TP, Bushnell D, Jagendorf AT (1993) Purified zinc protease of pea chloroplasts, EP1, degrades the large subunit of ribulose-1,5-bisphosphate carboxylase/oxygenase. Plant Physiol **103:** 585–591

Chen MH, Liu LF, Chen YR, Wu HK, Yu SM (1994) Expression of alpha-amylases, carbohydrate metabolism, and autophagy in cultured rice cells is coordinately regulated by sugar nutrient. Plant J **6:** 625–636

Chirgwin JJ, Przbyla AE, MacDonald RJ, Rutter WJ (1979) Isolation of biologically active ribonucleic acid from sources enriched in ribonuclease. Biochemistry **18:** 5294–5299

Clough SJ, Bent AF (1998) Floral dip: a simplified method for *Agrobacterium*-mediated transformation of *Arabidopsis thaliana*. Plant J **16:** 735–743

Funakoshi T, Matsuura A, Noda T, Ohsumi Y (1997) Analyses of APG13 gene involved in autophagy in yeast, *Saccharomyces cerevisiae*. Gene **192:** 207–213

Guiamet JJ, Pichersky E, Nooden LD (1999) Mass exodus from senescing soybean chloroplasts. Plant Cell Physiol **40:** 986–992

Hayashi M, Nito K, Toriyama-Kato K, Kondo M, Yamaya T, Nishimura M (2000) *At*Pex14p maintains peroxisomal functions by determining protein targeting to three kinds of plant peroxisomes. EMBO J **19:** 5701–5710

Hirai MY, Fujiwara T, Chino M, Naito S (1995) Effects of sulfate concentrations on the expression of a soybean seed storage protein gene and its reversibility in transgenic *Arabidopsis thaliana*. Plant Cell Physiol **36:** 1331–1339

Ichimura Y, Kirisako T, Takao T, Satomi Y, Shimonishi Y, Ishihara N, Mizushima N, Tanida I, Kominami E, Ohsumi M et al. (2000) A ubiquitin-like system mediates protein lipidation. Nature **408:** 488–492

Inada N, Sakai A, Kuroiwa H, Kuroiwa T (1998) Three-dimensional analysis of the senescence program in rice (*Oryza sativa* L.) coleoptiles: investigations by fluorescence microscopy and electron microscopy. Planta **206:** 585–597

Kabeya Y, Mizushima N, Ueno T, Yamamoto A, Kirisako T, Noda T, Kominami E, Ohsumi Y, Yoshimori T (2000) LC3, a mammalian homologue of yeast Apg8p, is localized in autophagosome membrane after processing. EMBO J **19:** 5720–5728

Kamada Y, Funakoshi T, Shintani T, Nagano K, Ohsumi M, Ohsumi Y (2000) Tor-mediated induction of autophagy via an Apg1 protein kinase complex. J Cell Biol **150:** 1507–1513

Kirisako T, Ichimura Y, Okada H, Kabeya Y, Mizushima N, Yoshimori T, Ohsumi M, Noda T, Ohsumi Y (2000) Reversible modification regulates the membrane-binding state of Apg8/Aut7 essential for autophagy and the cytoplasm to vacuole targeting pathway. J Cell Biol **151:** 263–276

Klionsky DJ, Ohsumi Y (1999) Vacuolar import of proteins and organelles from the cytoplasm. Annu Rev Cell Dev Biol **15:** 1–32

Liang XH, Jackson S, Seaman M, Brown K, Kempkes B, Hibshoosh H, Levine B (1999) Induction of autophagy and inhibition of tumorigenesis by *beclin 1*. Nature **402:** 672–676

Marty F (1978) Cytochemical studies on GERL, provacuoles, and vacuoles in root meristematic cells of *Euphorbia*. Proc Natl Acad Sci USA **75:** 852–856

Marty F (1999) Plant vacuoles. Plant Cell **11:** 587–599

Matile P (1975) The lytic compartment of plant cells. *In* Cell Biology Monographs, Vol 1. Springer-Verlag, Wien, Germany

Matile P, Winkenbach F (1971) Function of lysosomes and lysosomal enzymes in the senescing corolla of the morning glory. J Exp Bot **22:** 759–771

Matsuura A, Tsukada M, Wada Y, Ohsumi Y (1997) Apg1p, a novel protein kinase required for the autophagic process in *Saccharomyces cerevisiae*. Gene **192:** 245–250

McKinney EC, Ali N, Traut A, Feldmann KA, Belostotsky DA, McDowell JM, Meagher RB (1995) Sequence-based identification of T-DNA insertion mutations in *Arabidopsis*: actin mutants *act2-1* and *act4-1*. Plant J **8:** 613–622

Minamikawa T, Toyooka K, Okamoto T, Hara-Nishimura I, Nishimura M (2001) Degradation of ribulose 1,5-biphosphate carboxylase/oxygenase by vacuolar enzymes of senescing French bean leaves: immunocytochemical and ultrastructural observations. Protoplasma **218:** 144–153

Mizushima N, Noda T, Yoshimori T, Tanaka Y, Ishii T, George MD, Klionsky DJ, Ohsumi M, Ohsumi Y (1998a) A protein conjugation system essential for autophagy. Nature **395:** 395–398

Mizushima N, Sugita H, Yoshimori T, Ohsumi Y (1998b) A new protein conjugation system in human: the counterpart of the yeast Apg12p conjugation system essential for autophagy. J Biol Chem **273:** 33889–33892

Mizushima N, Yamamoto A, Hatano M, Kobayashi Y, Kabeya Y, Suzuki K, Tokuhisa T, Ohsumi Y, Yoshimori T (2001) Dissection of autophagosome formation using Apg5-deficient mouse embryonic stem cells. J Cell Biol **152:** 657–667

Moran R (1982) Formulae for determination of chlorophyllous pigments extracted with *N*,*N*-dimethylformamide. Plant Physiol **69:** 1376–1381

Moriyasu Y, Hillmer S (2000) Autophagy and vacuole formation. *In* DG Robinson, JC Rogers, eds, Vacuolar Compartments. Annu Plant Rev **5:** 71–89

Moriyasu Y, Ohsumi Y (1996) Autophagy in tobacco suspension-cultured cells in response to sucrose starvation. Plant Physiol **111:** 1233–1241

Musgrove JE, Elderfield PD, Robinson C (1989) Endopeptidases in the stroma and thylakoids of pea chloroplasts. Plant Physiol **90:** 1616–1621

Noda T, Kim J, Huang WP, Baba M, Tokunaga T, Ohsumi Y, Klionsky DJ (2000) Apg9p/Cvt7p is an integral membrane protein required for transport vesicle formation in the cvt and autophagy pathways. J Cell Biol **148:** 465–479

Oh SA, Lee SY, Chung IK, Lee CH, Nam HG (1996) A senescence-associated gene of *Arabidopsis thaliana* is distinctively regulated during natural and artificially induced leaf senescence. Plant Mol Biol **30:** 739–754

Ohsumi Y (2001) Molecular dissection of autophagy: two ubiquitin-like systems. Nat Rev Mol Cell Biol **2:** 211–216

Ohto M, Onai K, Furukawa Y, Aoki E, Araki T, Nakamura K (2001) Effects of sugar on vegetative development and floral transition in Arabidopsis. Plant Physiol **127:** 252–261

Ono K, Hashimoto H, Katoh S (1995) Changes in the number and size of chloroplasts during senescence of primary leaves of wheat grown under different conditions. Plant Cell Physiol **36:** 9–17

Park H, Eggink LL, Roberson RW, Hoober JK (1999) Transfer of proteins from the chloroplast to vacuoles in *Chlamydomonas reinhardtii* (chlorophyta): a pathway for degradation. J Phycol **35:** 528–538

Saito C, Ueda T, Abe H, Wada Y, Kuroiwa T, Hisada A, Furuya M, Nakano A (2002) A complex and mobile structure forms a distinct subregion within the continuous vacuolar membrane in young cotyledons of *Arabidopsis*. Plant J **29:** 245–255

Shimizu T, Inoue T, Shiraishi H (2001) A senescence-associated S-like Rnase in the multicellular green alga *Volvox carteri*. Gene **274:** 227–235

Shintani T, Mizushima N, Ogawa Y, Matsuura A, Noda T, Ohsumi Y (1999) Apg10p, a novel protein-conjugating enzyme essential for autophagy in yeast. EMBO J **18:** 5234–5241

Suzuki K, Kirisako T, Kamada Y, Mizushima N, Noda T, Ohsumi Y (2001) The pre-autophagosomal structure organized by concerted functions of APG genes is essential for autophagosome formation. EMBO **20:** 5971–5981

Tanaka K, Nakafuku M, Tamanoi F, Kaziro Y, Matsumoto K, Toh-e A (1990) IRA2, a second gene of *Saccharomyces cerevisiae* that encodes a protein with a domain homologous to mammalian ras GTPase-activating protein. Mol Cell Biol **10:** 4303–4313

Tanida I, Mizushima N, Kiyooka M, Ohsumi M, Ueno T, Ohsumi Y, Kominami E (1999) Apg7p/Cvt2p: A novel protein-activating enzyme essential for autophagy. Mol Biol Cell **10:** 1367–1379

Tanida I, Tanida-Miyake E, Ueno T, Kominami E (2001) The human homolog of *Saccharomyces cerevisiae* Apg7p is a protein-activating enzyme for multiple substrates including human Apg12p, GATE-16, GABARAP, and MAP-LC3. J Biol Chem **276:** 1701–1706

Thumm M, Egner R, Koch B, Schlumpberger M, Straub M, Veenhuis M, Wolf DH (1994) Isolation of autophagocytosis mutants of *Saccharomyces cerevisiae*. FEBS Lett **349:** 275–280

Thumm M, Kadowaki T (2001) The loss of *Drosophila APG4/AUT2* function modifies the phenotypes of *cut* and Notch signaling pathway mutants. Mol Genet Genom **266:** 657–663

Toyooka K, Okamoto T, Minamikawa T (2001) Cotyledon cells of *Vigna mungo* seedlings utilize at least two distinct autophagic machineries for degradation of starch granules and cellular components. J Cell Biol **154:** 973–982

Tsukada M, Ohsumi Y (1993) Isolation and characterization of autophagy-defective mutants of *Saccharomyces cerevisiae*. FEBS Lett **333:** 169–174

Vierstra RD (1996) Proteolysis in plants: mechanisms and functions. Plant Mol Biol **32:** 275–302

Wang CW, Kim J, Huang WP, Abeliovich H, Stromhaug PE, Dunn WA, Klionsky DJ (2001) Apg2 is a novel protein required for the cytoplasm to vacuole targeting, autophagy, and pexophagy pathways. J Biol Chem **276:** 30442–30451

Wittenbach VA, Lin W, Habert RR (1982) Vacuolar localization of proteases and degradation of chloroplasts in mesophyll protoplasts from senescing primary wheat leaves. Plant Physiol **69:** 98–102

Yoshida S, Ito M, Nishida I, Watanabe A (2001) Isolation and RNA gel blot analysis of genes that could serve as potential molecular markers for leaf senescence in *Arabidopsis thaliana*. Plant Cell Physiol **42:** 170–178